DOI : https://doi.org/10.56452/7-12-37

ISSN: 0974-5823 Vol. 7 No. 12 December, 2022

International Journal of Mechanical Engineering

To Study the Performance of Vortex Tube for Different Inert Gases using CFD

Amol Dhumal[1], Shivtej Karande[2], Manoj Jagdale[3], Naren Kate[4], Sonal Shamkuwar[5], Vijay Marathe[6]

[1,2,3,4,5]Department of Mechanical Engineering, Vishwakarma Institute of Information Technology, Pune, Maharashtra-411048, India.

[6]Department of Engineering and Applied Science, Vishwakarma Institute of Information Technology, Pune, Maharashtra-411048, India.

ABSTRACT

A counter flow vortex tube, commonly referred as a Vortex Tube [VT], is a device that generates cold and hot streams from a single high-pressure compressed air/gas intake. The objective of thisresearch is to understand how different inert gases affect the performance of VT. Computational/ Numerical analysis will give a better understanding of the effects on performance. For this numerical investigation approach, we chose Computational Fluid Dynamics (CFD) as a technique and flow is simulated using ANSYS FLUENT software. A simulated flow field in the VThelps to analyze the complex flow separation in the tube. The VT has been studied for different turbulentmodels such as Spalart Alarmas, Standard k-epsilonand Standard k- omega. CFD analysis shows that Standard k-ε model predicts better results. Further using the same turbulence model CFD analysis is done for different inert gases such as Helium, Argon, Neon. In comparison to other inert gases, helium asa working fluid provides the greatest temperature separation. This project will help to select the proper turbulence model and simulation results will be helpful to select the appropriate working fluid to obtain the required temperature difference with maximum efficiency.

KEYWORDS: Counter flow vortex tube Inert gases, Computational fluid dynamics Temperature separation, Cold mass fraction.

1. INTRODUCTION

A counter flow vortex tube is a mechanical device that divides a single compressed gas stream into two distinct hot and cold streams. There are nomoving parts in it. When a stream of compressed gas at room temperature is injected tangentially into the device, it first goes through a nozzle that is designed to flow the gas tangentiallywithin the tube, which aids in the formation of a high-speed tornado (vortex) movement inside the tube. A special conical-shaped control valve situated at the hot end of the tube allows some of the higher-temperature gas to escape while diverting the remaining gas back down the tube asa smaller inner vortex within the larger peripheral vortex. The second vortex then leaves the tube at the opposite end, at a lower temperaturethan the incoming gas.

While the outer vortex travels down one end of the tube and the inner vortex travels in the opposite direction, both rotate in the same angular direction and at the same angular velocity. Since the inner vortex has a smaller radius than the outer one, the conservation of angular

DOI : https://doi.org/10.56452/7-12-37

momentum states that it should rotate at a faster rate. Hence, work is done to change its angular momentum and rotate it at a small angular velocity than the outer vortex. As a result of interacting with the outer vortex flow, the inner vortex loses angular momentum and kinetic energy. This loss of kinetic energy leads to the heat transfer from the inner vortex to the outer vortex. As a result, the outer vortex on the periphery warms up while the inside vortex cools down.

The ratio of the mass of air going out through the cold exit to the actual mass of air entering the vortex tube through the inlet is known as the cold mass fraction. The control valve regulates the cold and hot mass flow rates, that is it ultimately controls the cold mass fraction. Cold mass fraction can be adjusted to change the temperature of the hot and cold streams. Cold mass fraction, Inlet pressure, and vortex tube geometry play an important role in temperature separation.

There are many advantages of this device. Since it has no moving mechanical moving parts, the maintenance cost is less, and this results in longer utility life. Moreover, it has no chemical reactions involved in the process of temperature separation. The temperature separation is a rapid action, it is produced instantaneously It has a wide range of applications due to such advantages: cooling machine components, cooling electronic control cabinets, chilling environmental chambers, refrigerators, cooling equipment in CNC machines, heating processes, and so on. Vortex tubes are specifically used in the manufacturing industry to cool cutting tools. As most machine shops already produce compressed air, the vortex tube is well-suited for the above uses. Vortex tube is small and light, and it does not require Freon or other types ofrefrigerants. So, VT fully removes or significantly decreases the requirement of costly dangerous liquid coolant.

Vortex tubes are commonly used in lathe operations, cutting, drilling, boring, milling, grinding, and other precision machining operationsincluding both manually and CNC machines. Dry compressed air is needed to clean the cutting tool and cutting edges, and a paint booth requires compressed air for painting manufactured components. CNC machines (without manual control and coding) are all operated on compressedair.

Many studies and research are being performed in order to examine and forecast the performance ofthe vortex tube for various features or characteristics, since the issue of vortex tubes has piqued the researchers' attention. Researchers find it challenging to perform an experimental study andassess the data when research becomes more complex. So in such cases, CFD can be used to derive flow results inside the vortex tube for various parameters. The simulations conducted in CFD are less time-consuming and require less cost for getting the results than conducting experiments.When used systematically, CFD can be a good substitute for experimental studies. There are many2-D and 3-D models in CFD that replicates general fluid dynamics within the vortex tubes.

2. LITERATURE REVIEW AND OBJECTIVES

Recently as the computational fluid dynamics (CFD) field gets wider and more user-friendly. It's now being widely used to explain the phenomenon of energy separation within the vortex tube.

Frohlingsdorf et al. used a CFD solver to describe the vortex tube flow, which includes compressible and turbulent effects. Secchiaroli et al. [1] successfully applied RSM (Reynolds Stress Model) in a 2D axisymmetric computational model of the vortex tube for the first time. On a commercial vortex tube, Skye et al [2] conducted an experimental and CFD research. The authors used roughly 25,000 cells to create a two- dimensional CFD model of a vortex tube.

Shamsoddini et al. [3] found that the axisymmetric CFD model could forecast the flow structure of a vortex tube with numerous inlet nozzles quite well.

Aydin and Baki [4] conducted an experiment employing Air, O2, and N2 as working gases for a vortex tube and found that Nitrogen provided the best temperature separation. Dutta et al. [5] used CFD to analyse a 2D axisymmetric model of a vortex tube with over 40,000 cells for various turbulence models, including Standard k-, RNG k-, Standard k-u, and SST k-u, and found that the temperature separation predicted by CFD was reasonably close to experimental observations.

CFD analysis carried out on a 2D model of a counter-flow vortex tube for different gases Air, N2, CO2, O2 by H.R. Thakare and A.D. Parekh [6] The temperature separation graph was plotted with respect to cold mass fraction, and it was found to be lowest when CO2 was present.

3. MATHEMATICAL MODELLING

Fluent's pressure-based solver is used to solve the governing equations of continuity, momentum, andenergy.

3.1 Governing Equations of CFD:

The following are the CFD governing equationsthat are studied in this project.

a. Continuity Equation:

$$\frac{\partial \rho}{\partial t} + V(\rho v) = s_m$$

b. Momentum Equation:

$$\frac{\partial(\rho\,\vec{v}\,)}{\partial x} + \nabla.(\rho\,\vec{v}\vec{v}) = -\nabla p + \nabla.\tau + \rho\,\vec{g} + \vec{F}$$

c. Energy Equation:

$$\frac{\partial \rho h_0}{\partial x} - \frac{\partial P}{\partial t} + div(\rho h u) = div(\lambda grad T)$$

d. Equation of state:

$$\boldsymbol{P = \rho R T_S}$$

Some other additional Transport equations are alsoused.

3.2 Transport Equations of Various Models:

3.2.1 Spalart-Allmaras model:

Gk stands for turbulent viscosity production. The molecular kinematic viscosity is denoted by ν.

The degradation of turbulent viscosity in the near-wall area is referred to as Yv.

DOI : https://doi.org/10.56452/7-12-37

Constants: - Sv and Cb2

$$\frac{\partial(\rho\,\tilde{v})}{\partial t} + \frac{\partial(\rho\,\tilde{v}\,u_i)}{\partial x_i} = G_v + \frac{1}{\sigma\tilde{v}}\left[\frac{\partial}{\partial x_j}\left\{(\mu + \rho\tilde{v})\frac{\partial\tilde{v}}{\partial x_j}\right\} + C_{b2}\rho\left(\frac{\partial\tilde{v}}{\partial x_j}\right)\right] - Y_v + S_{\tilde{v}}$$

3.2.2 Standard k-ε model:

The k-model is concerned with the mechanisms that influence turbulent kinetic energy. The turbulent viscosity is assumed to be isotropic.

$$\frac{\partial(\rho k)}{\partial t} + \frac{\partial(\rho k u_i)}{\partial x_i} = \frac{\partial}{\partial x_j}\left[\left(\mu + \frac{\mu_t}{\sigma_k}\right)\frac{\partial k}{\partial x_j}\right] + G_k + G_b - \rho\varepsilon - Y_m + S_k$$

$$\frac{\partial(\rho\varepsilon)}{\partial t} + \frac{\partial(\rho\varepsilon u_i)}{\partial x_i} = \frac{\partial}{\partial x_j}\left[\left(\mu + \frac{\mu_t}{\sigma_\varepsilon}\right)\frac{\partial\varepsilon}{\partial x_j}\right] + C_{13}\frac{\varepsilon}{k}(G_k + C_{3\varepsilon}G_b) - C_{2\varepsilon}\rho\frac{\varepsilon^2}{k} + S_\varepsilon$$

The creation of turbulent kinetic energy due to mean velocity gradients is represented by Gk.

Gb is the buoyancy-induced creation of turbulent kinetic energy.

The contribution of fluctuating dilatation in compressible turbulence to the overall dissipation rate is represented by YM.

Constants: - C1ε, C2ε, C3ε

The turbulent Prandtl numbers are Sk and S.

3.2.3 Standard k-m model:

It's applied to compute low-Reynolds-number effects, compressibility, and shear flow spreading adjustments.

$$\frac{\partial(\rho k)}{\partial t} + \frac{\partial(\rho k u_i)}{\partial x_i} = \frac{\partial}{\partial x_j}\left[\Gamma_k\frac{\partial k}{\partial x_j}\right] + G_k - Y_k + S_k$$

$$\frac{\partial(\rho\omega)}{\partial t} + \frac{\partial(\rho\omega u_i)}{\partial x_i} = \frac{\partial}{\partial x_j}\left[\Gamma_\omega\frac{\partial\omega}{\partial x_j}\right] + G_\omega - Y_\omega + S_\omega$$

Gu denotes the generation of u, whereas Gk and Gu denote the effective diffusivity of k and u.

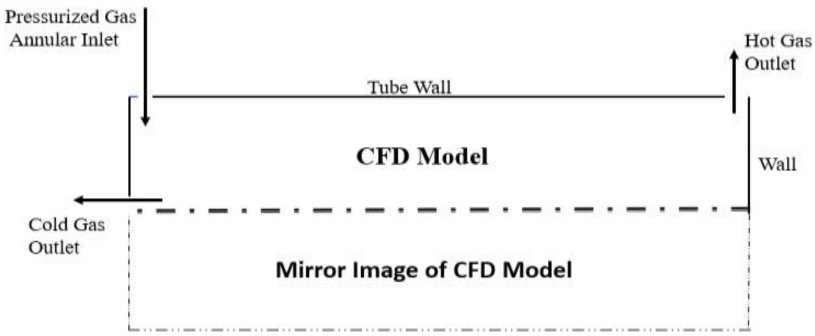

Figure 1 Schematic diagram symmetric CFD model is show for clarification

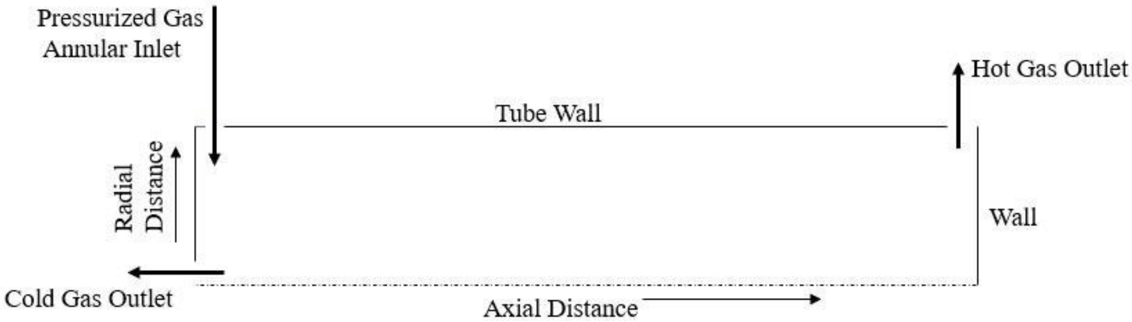

Figure 2 Schematic diagram of axisymmetric computational domain of vortex tube of Skye et al. [2]

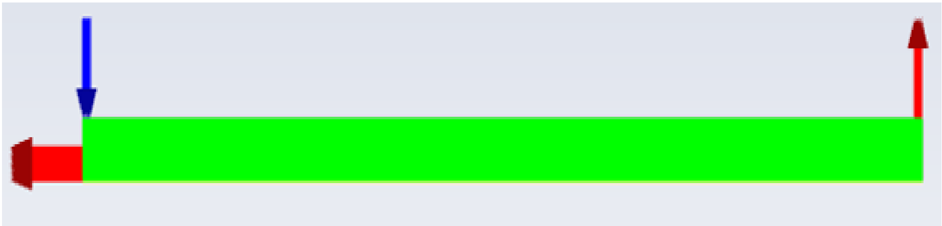

Figure 3 Shown schematic is axisymmetric model in CFD Fluent showing inlets, outlet and computational domain

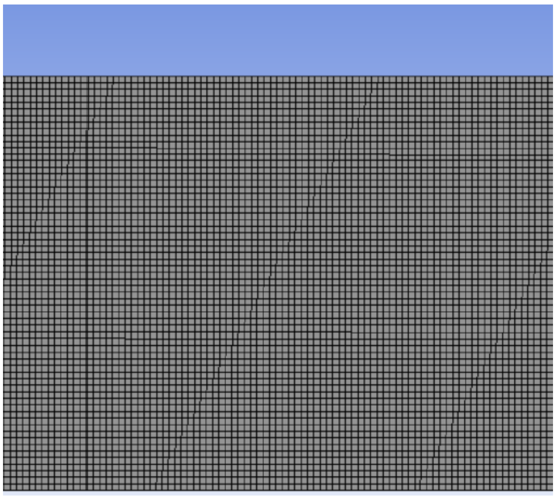

Figure 4 Part of vortex tube showing structured mesh

DOI : https://doi.org/10.56452/7-12-37

4. BOUNDARY CONDITIONS

The boundary conditions that were used in the current CFD simulation are described here. Skye et al. [2] employed a vortex tube with an inner diameter of 11.4mm and an operational length of 106mm in their experimental study. The working fluid was air, which was injected at a pressure of around 4.68 bar [2]. The diameter of the cold end was 6.2 mm. The air flowed into the vortex tube through 6 separate nozzles in the original laboratory experiment. The inlet has been represented Figure 2 as an annular inlet in this CFD model, following the same technique as Skye et al. [2]. The 2D computational domain used in the present study has been shown in Fig. 1(a). which is modelled using the mentioned dimensions in Skye et al. [2] as shown in Figure 1

Figure 4 illustrates the structured fine mesh employed in this investigation. To create structured cells with more than 75000 cells, very fine meshing is done. CFD simulations were performed with this many cells, yielding more accurate results. Since the 2D model keeps the same three-dimensional aspects of the computational domain [7] ,it is chosen over 3D to save additional computational efforts as well as time refer Figure 3. A pressure- based implicit solver was used to run all CFD simulations in steady-state mode. The flow

inside the vortex tube is compressible as it is gaseous in the state. Hence, the ideal gas assumption has been used in the analysis.

The vortex tube's inlet is given the boundary condition of mass flow inlet, with mass flow rate of 0.00835 kg/s, radial and tangential components of velocity of 0.25, 0.97, and inlet room temperature of 294.2 K, respectively. With no-slip boundary conditions, the vortex tube's wall is believed to be stationary and adiabatic Skye et al. [4] carried out experimental research that achieved these values. Pressure outlets include the hot end and the cold end. Because the cold end is open to the atmosphere, zero gauge pressure is considered as a boundary condition. For Pressure-Velocity Coupling, a SIMPLE algorithm was applied. Under Relaxation Factors are the preset standard values. The convergence conditions were defined using default residual values of the order of 10-6 for energy and 10-3 for all other parameters.

Air is used as a working fluid throughout the validation and also during the analysing different turbulent models.The properties of air areconsidered throughout the validation study are:-cp = 1006.43 J/kg. K,

k =0.0242 W/m.K, M = 28.966 kg/kmol, m = 1.7894×10^{-5} kg/ m.s [6]

Table 1 Comparison of different studies for deviation of minimum total temperature of cold end predicted.

Sr. No.	**CFD study by**	**Min (Tc)exp**	**Max (DTc)exp=Tin-Min. (Tc)exp**	**Min (DTc)cfd**	**Max.= (DTc)Tin - Min (Tc)cfd**
1.	Skye et al., Standard k-ε[2]	251.3 K	294.2 – 251.3 = 42.9 K	265.2 K	294.2 - 265.2= 29 K
2.	H.R. Thakare and Parekh [6]	251.3 K	294.2 – 251.3 = 42.9 K	254.5 K	294.2 – 254.5 = 39.7 K
3.	Farouk andFarouk [7]	251.3 K	294.2 – 251.3 = 42.9 K	256.2 K	294.2 – 256.2 = 38 K

DOI : https://doi.org/10.56452/7-12-37

4.	Pourmahmoud and Akhesmeh, Standard k-ε [8]	251.3	294.2 – 251.3 = 42.9 K	256.9 K	294.2 – 256.9 = 37.3 K
5.	Standard k-ε[Present]	251.3 K	294.2 – 251.3 = 42.9 K	256.16 K	294.2 – 256.16 =38.04

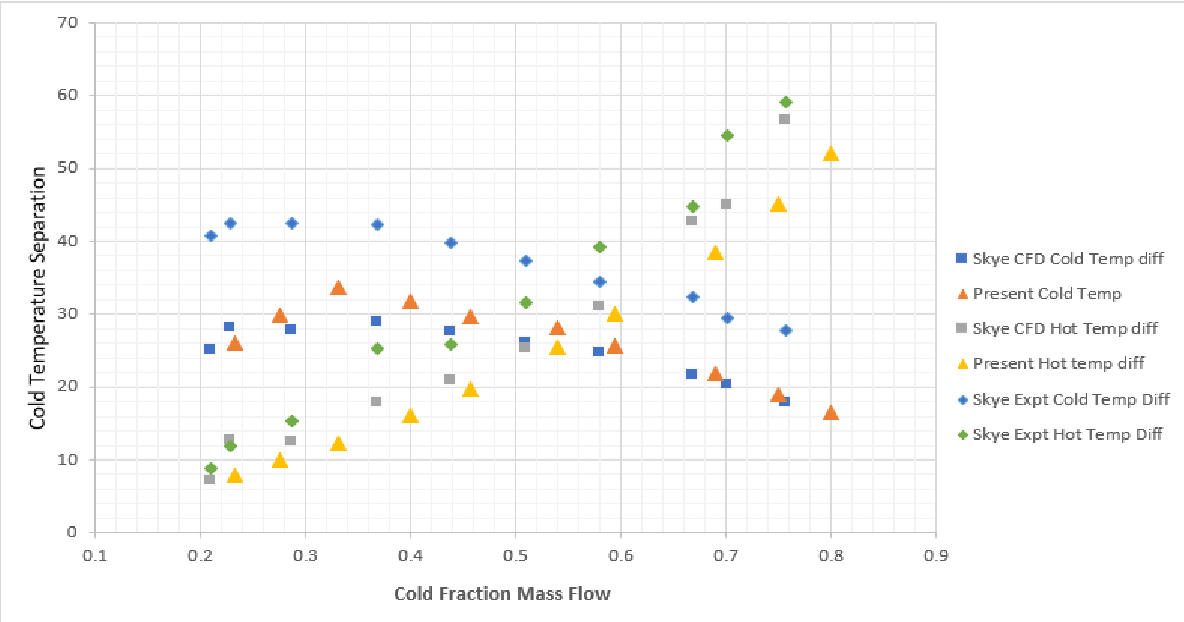

Figure 5 Comparison of present CFD results with the experimental and CFD results of Skye et al. [2]

5. VALIDATION

The current CFD model's results are compared to Skye et al experimental and CFD results [2]. As displayed in Figure 5, the results of the current CFD investigation accord better with the results of Skye et al. [2]'s experiments. The observed results Table 1 are also consistent with Farouk and Farouk [7] and Pourmahmoud and Akhesmeh [8] CFD results. It indicates that the simulation methodology used in this work is appropriate, and the model is trustworthy for further research. Figure 6 illustrates the contours of the entire temperature distribution inside the vortex tube. The temperature separation phenomena clearly demonstrate that the temperature of the central axial flow leaving from the cold end is much lower than the temperature of the incoming fluid. The temperature separation phenomena clearly demonstrate that the temperature of the centra axial flow leaving from the cold end is much lower than the temperature of the incoming fluid. Simultaneously, the circumferential flow is hotter than the central flow, with the highest temperature near the hot end.

The impact of various parameters on temperature separation may now be investigated using such a trustworthy model. This model has been studied to determine the magnitude of temperature separation depending on: -

a. At various cold mass fraction values

b. Turbulence Models, such as Spalart Allmaras, Standard k-, and Standard k-omega.

DOI : https://doi.org/10.56452/7-12-37

c. Different Inert Gases as a working gas i.e., Helium, Neon, and Argon.

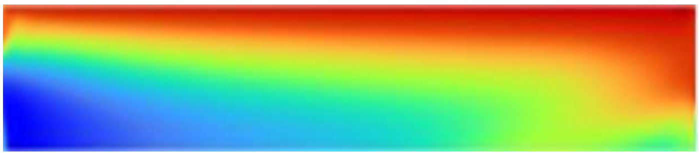

Figure 6 CFD analysis shows the total temperature contour

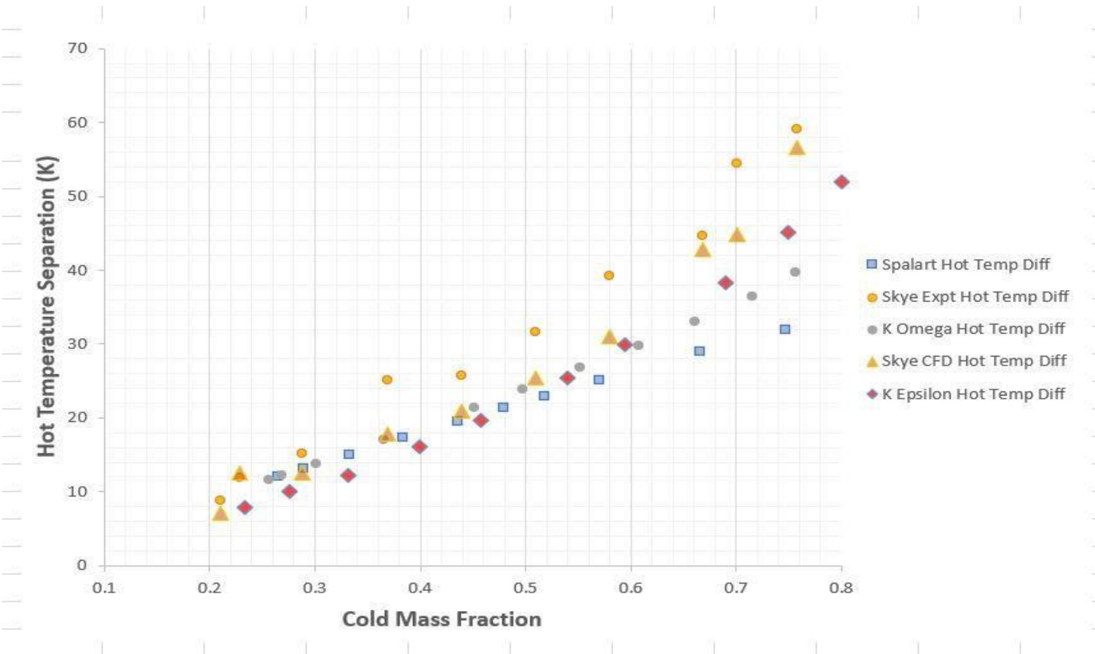

Figure 7 Different turbulence models predict hot end temperature separation.

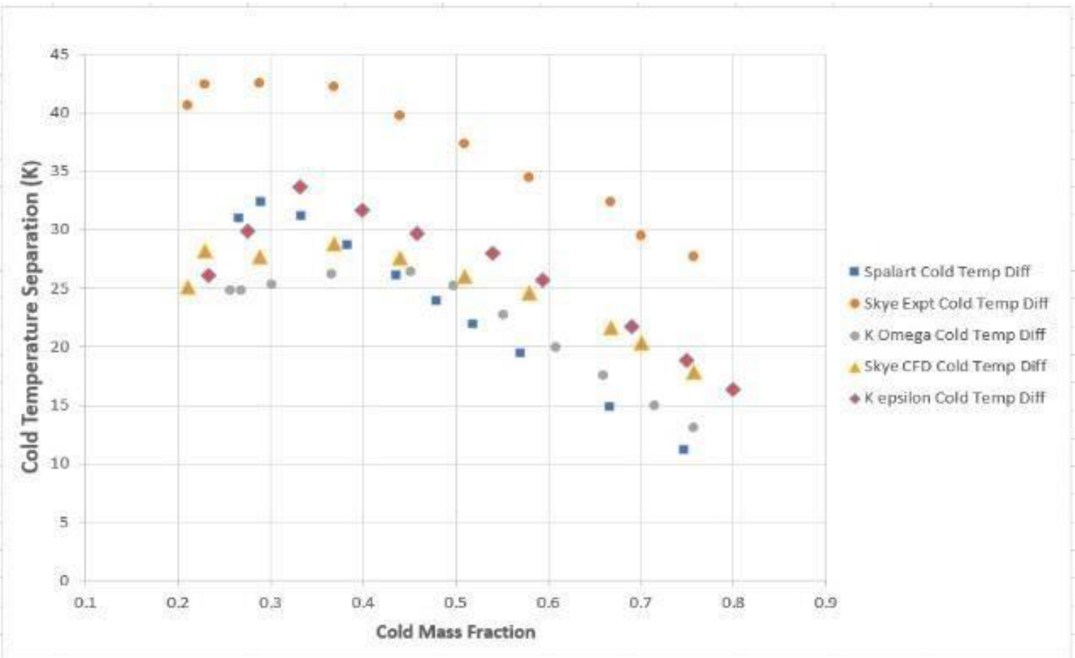

Figure 8 Different turbulence models predict cold end temperature separation.

DOI : https://doi.org/10.56452/7-12-37

6. RESULTS

The results obtained are discussed in this section. This includes impact of different turbulence models as well as the effects of various inert gases.

6.1 Effect of turbulence model on the vortex tube performance

In this paper, we have considered different turbulence models to differentiate the temperature separation magnitude variation. These results are taken from Fluent software and graphs are drawn.

Here, Spalart, Skye, K Omega, and K epsilon models are considered, also Skye CFD temperature difference is also given for comparison. H.M. Skye [2] underlines the temperature difference with respect to a cold fraction. The Cold Temperature separation is the difference measured at the cold inlet and the hot temperature separation is the difference measured at the hot outlet of the vortex tube.

In comparison to experimental results, the Standard k-w model underpredicts the cold end temperature difference for cold mass fractions less than 0.35. Up to a cold mass fraction of 0.35, the Spalart Allmaras model matches experimental results well. The outcomes then begin to diverge. The experimental results are more consistent with the Standard k-results model.

The graph of Figure 7 Cold Temperature Difference with regard to Cold Mass Fraction K epsilon model indicates maximum Cold Temperature separation in the graphs Figure 8. The K epsilon model also has the largest temperature separation for the Hot Temperature Difference. The temperature is seen to increase up to a value and then decrease with rising cold mass Fraction in cold temperature separation with regard to cold mass fraction. In another graph, Figure 8 the hot end difference in temperature continues to grow in relation to the cold mass fraction. The temperature separation for the K epsilon model is the largest, while it is the smallest for the Spalart model.

Here, Spalart, Skye, K Omega, and K epsilon models are considered, also Skye CFD temperature difference is also given for comparison. H.M. Skye [2] underlines the temperature difference with respect to a cold fraction. The Cold Temperature separation is the difference measured at the cold inlet and the hot temperature separation is the difference measured at the hot outlet of the vortex tube.

In comparison to experimental results, the Standard k-w model underpredicts the cold end temperature difference for cold mass fractions less than 0.35. Up to a cold mass fraction of 0.35, the Spalart Allmaras model matches experimental results well. The outcomes then begin to diverge. The experimental results are more consistent with the Standard k-results model.

The graph of **Figure *7*** Cold Temperature Difference with regard to Cold Mass Fraction K epsilon model indicates maximum Cold Temperature separation in the graphs **Figure 8**. The K epsilon model also has the largest temperature separation for the Hot Temperature Difference. The temperature is seen to increase up to a value and then decrease with rising cold mass Fraction in cold temperature separation with regard to cold mass fraction. In another graph, **Figure 8** the hot

end difference in temperature continues to grow in relation to the cold mass fraction. The temperature separation for the K epsilon model is the largest, while it is the smallest for the Spalart model.

6.2 Impact of Different Inert Gases on Performance of Vortex Tube

As we know vortex tube is generally used for changing the temperature of air. We used different

DOI : https://doi.org/10.56452/7-12-37

inert gases i.e., Helium, argon and neon and noted down the changes with respect to various axial locations ranging from position near the stationary wall i.e., x/L= 0.1 to core portion of vortex tube i.e., at x/L =0.5 These changes are visualized using excel graphs in which the blue, gray and red dotted lines represent the variations for Helium, Argon and Neon gases respectively. In comparison to [6] these CFD results are determined to be qualitatively correct. [6] Inside the vortex tube, they present a radial profile of fluctuation in static temperature, swirl velocity, and axial velocity of diverse gases. With gases like nitrogen, CO2, and air, they looked at different thermophysical properties including thermal diffusivity and thermal conductivity.

6.2.1 Variations in Static Temperature: - Radial Profiles at Different Dimensionless Axial Locations:

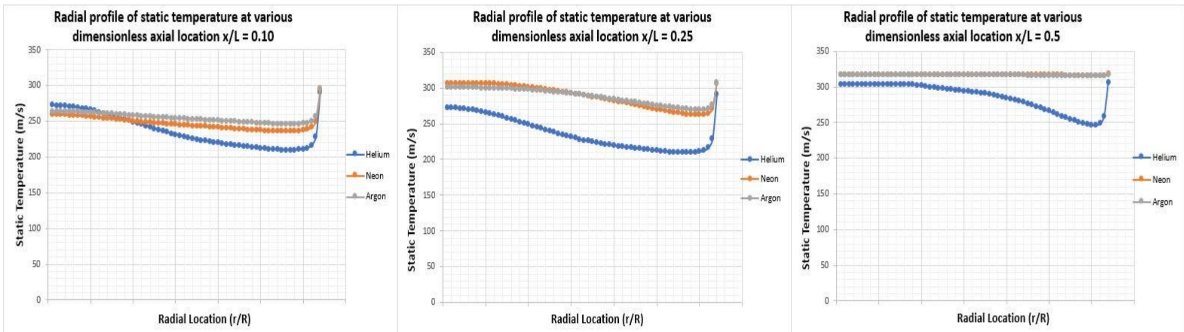

(a)

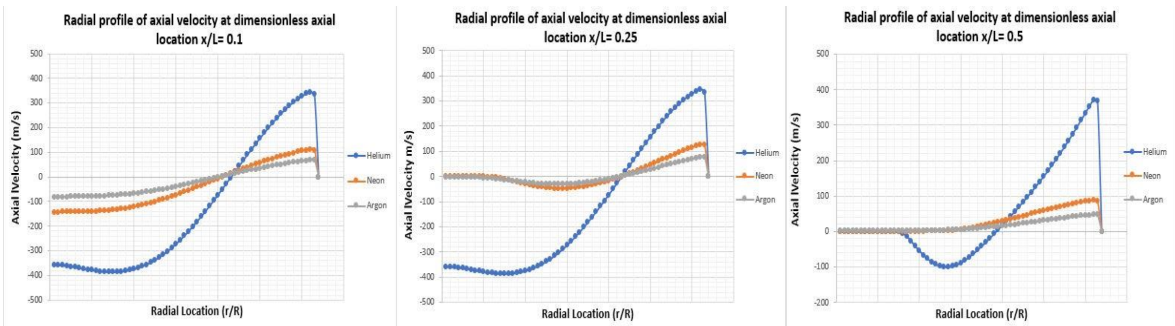

(b)

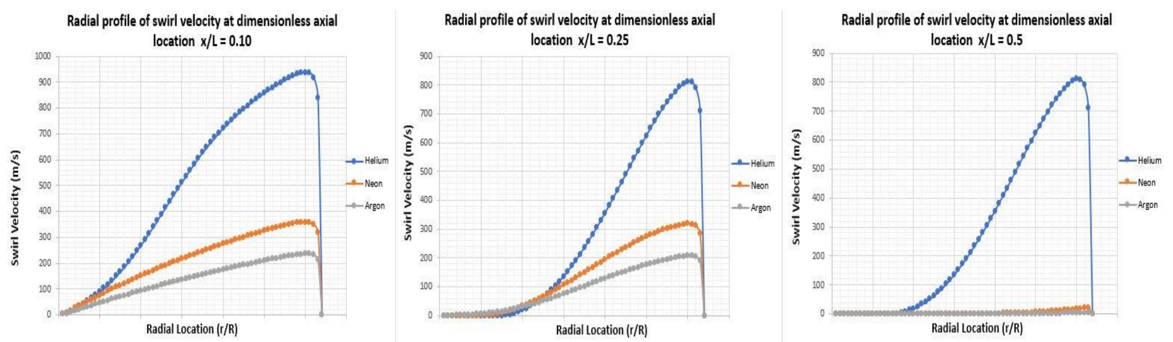

(c)

Figure 9 Radial profile of static temperature, axial velocity, swirl velocity for different inert gases at different dimensionless axial locations

DOI : https://doi.org/10.56452/7-12-37

6.2.2 Variations in Swirl Velocity: - Radial Profiles at Different Dimensionless Axial Locations:

Swirl is tangential flow component of a velocity vector. Here, variation in Swirl velocity is considered as a parameter for comparison between gases with respect to different axial positions, we can see the difference with the help of Figure 2 It depicts the fluctuation in inert gas swirl velocity at various dimensionless axial positions, along the radius of the vortex tube. At Figure 9 (b), Helium has the maximum swirl velocity in accordance with all the dimensionless axial locations of 2D geometry and Argon has lowest Swirl velocity at all locations. The Neon gas has its swirl velocity in between. From the graphs we can see that the swirl velocity increases with respect to axial location until the core of vortex tube.

For all studied inert gases, these profiles illustrate that gas flow at the core of the vortex tube is forced flow. As the flow goes from cold end to hot end, or with variable axial location, the magnitude of swirl velocity of gases increases.

Energy is compared to the swirl velocity distribution; it is found helium has the greatest energy separation. High swirl velocity indicates that the inside the tube expands more and has a lower static temperature. Helium has the largest swirl velocity, whereas Argon has the lowest, resulting in a higher magnitude of energy

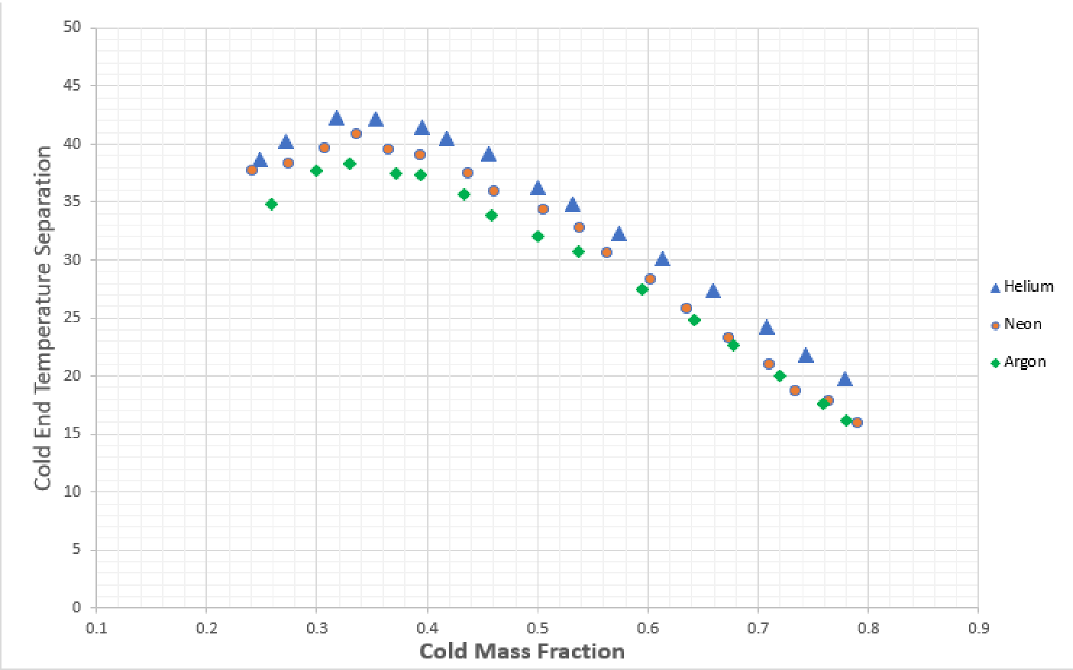

Figure 10 Cold end temperature separation predicted for different inert gases

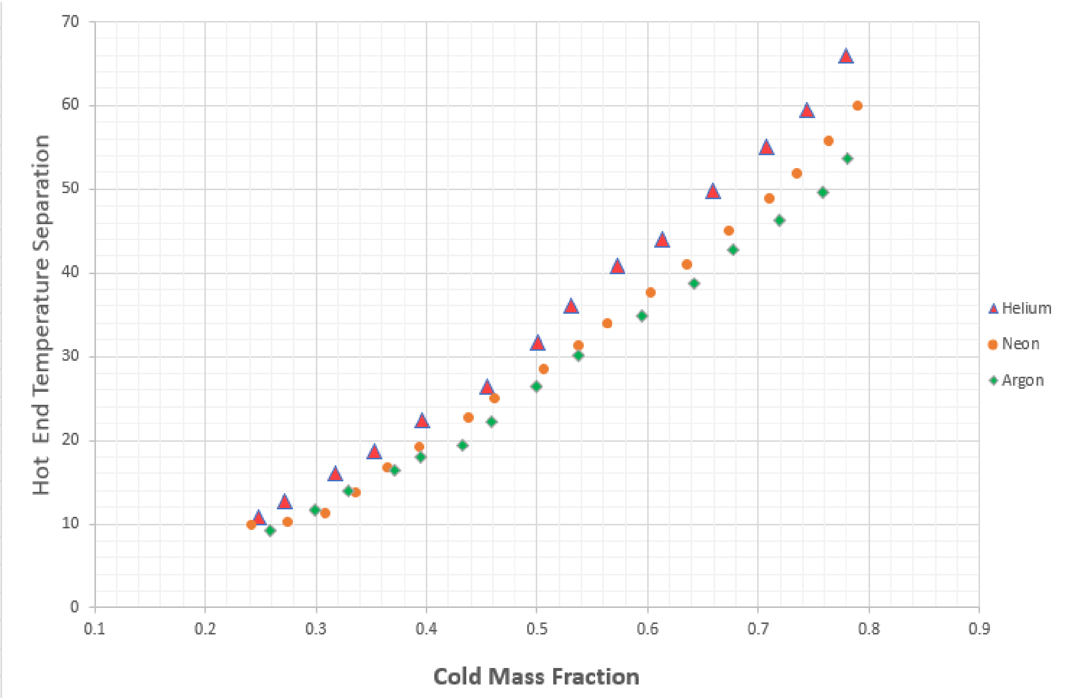

Figure 11 Hot end temperature separation predicted for different inert gases

6.2.3 Variations in Axial Velocity:- Radial Profiles at Different Dimensionless Axial Locations:\

Axial velocity is velocity along the x axis in translational direction. **Figure 9 (c)** depicts axial velocity variations in the vortex tube at different axial(longitudinal) locations. For almost all of the gases studied, the graph follows a similar trend of positive to negative magnitude. Helium has the largest axial velocity fluctuation, while Argon has the smallest.

We can see the reversal of flow takes places for all the inert gases, considering the negative and positive values of axial velocities. The drag force induced dur to the difference in pressures between the cold end & the flow inside the vortex tube acts on the gas particles as they migrate towards the hot end. If gas particles do not have enough energy to overcome the drag force, their velocities fall to zero, and the gas expands. As the temperature of the gas decreases due to expansion, the gas particle gains axial velocity toward the cold end. Because of the pressure differential, the gas particle accelerates, increasing it's own axial velocity near the cool end. Helium has the highest axial velocity in both positive and negative axes.

As with other flow characteristics, the axial velocity of Neon and Argon is near to each other.

The axial velocities in Argon and Neon vary in similar fashion. For x/L=0.25 velocity first decreases and then increases for Argon and Neon. At x/L=0.5 helium doesn’t show variation until some portion of the graph but then proceeds to follow the similar pattern like other locations i.e., negative to positive magnitude.

Comparing both Figure 10 and Table 2 shows that as the value of specific heat increases, the magnitude of temperature increases

at constant pressure. It's also important to note that as molecular weight decreases, temperature separation increases. Here it is not possible to do analysis like [9] performed based on the specific heat capacity ratio because all the inert gases have same specific heat capacity ratio as they are monotonic in nature. Neon, Argon have the nearly close values of specific heat at constant pressure, so, they are expected to have the nearly same energy separation.

DOI : https://doi.org/10.56452/7-12-37

6.2.4 Effect Of inert gases on temperatureseparation:

Figure 10 shows the temperature separation between the cold and hot ends of the vortex tube as the cold mass fraction increases. It shows that when helium is employed as a working gas inside a vortex tube, the cold and hot temperature difference is greatest, while it is smallest for argon. For all gases, the value of cold temperature separation decreases as the cold mass fraction increases. For example, as the cold mass fraction grows, the hot temperature difference grows. Figure 4 depicts the trend of growth.

Helium has the highest temperature separation, as seen in graph Figure 10, which is due to its maximum specific heat at constant pressure and smallest molecular weight. Comparing both Figure 10 and Table 2 shows that as the value of specific heat increases, the magnitude of temperature increases

at constant pressure. It's also important to note that as molecular weight decreases, temperature separation increases. Here it is not possible to do analysis like [9] performed based on the specific heat capacity ratio because all the inert gases have same specific heat capacity ratio as they are monotonic in nature. Neon, Argon have the nearly close values of specific heat at constant pressure, so, they are expected to have the nearly same energy separation.

7. CONCLUSIONS

The purpose of the CFD simulation of the vortextube was to figure out:

a. The cold mass fraction effect
b. Effect of variety of turbulence models
c. The impact of various inert gases

The following conclusions can be drawn from thecurrent CFD research:

1. The temperature separation effect reported from the current CFD study matches experimental data.
2. The extent of temperature separation was shownto be vary for different turbulence models.
3. For the range of cold mass fraction, the results ofthe Standard k-model are consistent.
4. Of the inert gases tested, Helium has the highestmagnitudes of both hot and cold end temperature separation, whereas Argon and Neon have relatively similar magnitudes.
5. Helium has the greatest temperature separationdue to its low molar mass and low specific heat value at constant pressure. As a result, it can be stated that gases with low molar mass and low
6. specific heat have a greater energy separation effect than gases with higher respective values.

NOMENCLATURE

cp	Specific heat at constant pressure (kJ/kgk),
T	Temperature (K),
ΔT	Temperature drop (K),
ν	Transported variable in the Spalart–Allmaras model,
ε	Dissipation rate of kinetic energy,
Ts	Static temperature (K),
Tc	cold end temperature (K),
DTc	cold end temperature separation (K)
Th	hot end temperature, (K)
V	Velocity magnitude (m/s)
x	axial distance from left end of the vortextube (mm)
K	Kelvin
k	thermal conductivity (W/ m. K),
L	total length of vortex tube (mm) ,
D	Vortex tube diameter (m),
M	molecular weight, (kg/ kmol)
m	mass flow rate of fluid, (kg/s

REFERENCES

[1] Secchiaroli, A., Ricci, R., Montelpare, S. and D'alessandro, V., 2009. Numerical simulation of turbulent flow in a Ranque–Hilsch vortex tube. International Journal of Heat and Mass Transfer, 52(23-24), pp.5496-5511.

[2] Skye, H.M., Nellis, G.F. and Klein, S.A.,2006. Comparison of CFD analysis to empirical data in a commercial vortex tube. International journal of refrigeration, 29(1), pp.71-80.

[3] Thakare, H.R. and Parekh, A.D., 2015. Computational analysis of energy separation in counter—flow vortex tube. Energy, 85, pp.62-77.

[4] Shamsoddini, R. and Nezhad, A.H., 2010. Numerical analysis of the effects of nozzles number on the flow and power of cooling of a vortex tube. International journal of refrigeration, 33(4), pp.774-782.

[5] Aydın, O. and Baki, M., 2006. An experimental study on the design parameters of a counterflow vortex tube. Energy, 31(14), pp.2763-2772.

[6] Dutta, T., Sinhamahapatra, K.P. and Bandyopdhyay, S.S., 2010. Comparison of different turbulence models in predicting the temperature separation in a Ranque– Hilsch vortex tube. international journal of refrigeration, 33(4), pp.783-792.

[7] Farouk, T. and Farouk, B., 2007. Large eddy simulations of the flow field and temperature separation in the Ranque– Hilsch vortex tube. International Journal of Heat and Mass Transfer, 50(23-24), pp.4724-4735.

DOI : https://doi.org/10.56452/7-12-37

[8] Pourmahmoud, N. and Akhesmeh, S., 2008, July. Numerical investigation of the thermal separation in a vortex tube. In Proceedings of world academy of science, engineering and technology (Vol.33, pp. 409-415)

[9] Khazaei, H., Teymourtash, A.R. and Malek-Jafarian, M., 2012. Effects of gas properties and geometrical parameters on performance of a vortex tube. Scientia Iranica, 19(3), pp.454-462.

[10] .FLUENT 6.3, theory. Fluent Inc.; September 2006

[11] Cengel YA. Heat transfer: a practical approach. 2nd ed. McGraw-Hill; 2003. p.23. ISBN 0072458933.